



HAL
open science

Shape diagrams for 2D compact sets - Part II: analytic simply connected sets.

Séverine Rivollier, Johan Debayle, Jean-Charles Pinoli

► **To cite this version:**

Séverine Rivollier, Johan Debayle, Jean-Charles Pinoli. Shape diagrams for 2D compact sets - Part II: analytic simply connected sets.. Australian Journal of Mathematical Analysis and Applications, 2010, 7 (2), Article 4, pp. 1-21. hal-00550950

HAL Id: hal-00550950

<https://hal.science/hal-00550950>

Submitted on 18 Jan 2011

HAL is a multi-disciplinary open access archive for the deposit and dissemination of scientific research documents, whether they are published or not. The documents may come from teaching and research institutions in France or abroad, or from public or private research centers.

L'archive ouverte pluridisciplinaire **HAL**, est destinée au dépôt et à la diffusion de documents scientifiques de niveau recherche, publiés ou non, émanant des établissements d'enseignement et de recherche français ou étrangers, des laboratoires publics ou privés.

SHAPE DIAGRAMS FOR 2D COMPACT SETS - PART II: ANALYTIC SIMPLY CONNECTED SETS

S. RIVOLLIER, J. DEBAYLE AND J.-C. PINOLI

ABSTRACT. Shape diagrams are representations in the Euclidean plane introduced to study 3-dimensional and 2-dimensional compact convex sets. However, they can also be applied to more general compact sets than compact convex sets. A compact set is represented by a point within a shape diagram whose coordinates are morphometrical functionals defined as normalized ratios of geometrical functionals. Classically, the geometrical functionals are the area, the perimeter, the radii of the inscribed and circumscribed circles, and the minimum and maximum Feret diameters. They allow twenty-two shape diagrams to be built. Starting from these six classical geometrical functionals, a detailed comparative study has been performed in order to analyze the representation relevance and discrimination power of these twenty-two shape diagrams. The first part of this study is published in a previous paper [16]. It focused on analytic compact convex sets. A set will be called analytic if its boundary is piecewise defined by explicit functions in such a way that the six geometrical functionals can be straightforwardly calculated. The purpose of this paper is to present the second part, by focusing on analytic simply connected compact sets. The third part of the comparative study is published in a following paper [17]. It is focused on convexity discrimination for analytic and discretized simply connected compact sets.

1 INTRODUCTION

The Santalo's shape diagrams [18] allow to represent a 2D compact convex set by a point in the Euclidean 2D plane from six geometrical functionals: the area, the perimeter, the radii of the inscribed and circumscribed circles, and the minimum and maximum Feret diameters [6]. The axes of each shape diagram are defined from a pair of geometric inequalities relating these functionals. Sometimes, the two geometric inequalities provide a complete system: for any range of numerical values satisfying them, there exists a compact convex set with these values for the geometrical functionals (in other words, a point within the 2D Santalo shape diagram describes a 2D compact convex set). This is not valid for all the Santalo shape diagrams.

This paper deals with the study of shape diagrams for a wide range of 2D non-empty analytic simply connected compact sets. The first part [16] of this study focused on the compact convex sets. This second part generalizes to the simply connected compact sets. The considered simply connected compact sets are mapped onto points in these shape diagrams, and through dispersion and overlapping quantifications, the shape diagrams are classified according to their ability to discriminate the simply connected compact sets.

Key words and phrases. Analytic simply connected compact sets, Geometrical and morphometrical functionals, Shape diagrams, Shape discrimination.

2 SHAPE FUNCTIONALS

In this paper, the non-empty analytic simply connected compact sets in the Euclidean 2-space \mathbb{E}^2 are considered. A set will be called analytic if its boundary is piecewise defined by explicit functions in such a way that the geometrical functionals enumerated below can be calculated. These geometrical functionals are determined in order to characterize the sets. They are related by the so-called geometric inequalities, which allow to define morphometrical functionals.

2.1 Geometrical functionals For a simply connected compact set in \mathbb{E}^2 , let A , P , r , R , ω , d , denote its area, its perimeter, the radii of its inscribed and circumscribed circles, its minimum and maximum Feret diameters [6], respectively. Figure 2.1 illustrates some of these geometrical functionals.

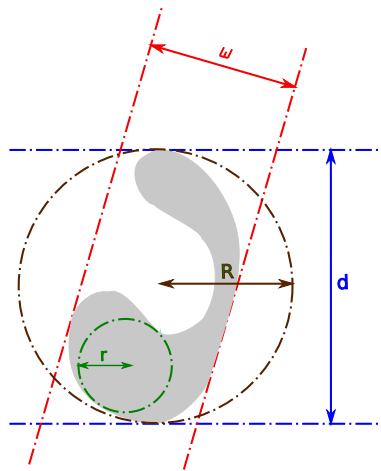


Figure 2.1: Geometrical functionals of a simply connected compact set: radii of inscribed (r) and circumscribed (R) circles, minimum (ω) and maximum (d) Feret diameters.

For a simply connected compact set, these six geometrical functionals are greater than zero. The line curves provide null values for A , r and ω , and the points for P , R and d . The sets with an infinite perimeter (the fractal sets) are not considered. P must be computed by a line integral.

2.2 Geometric inequalities For a simply connected compact set in \mathbb{E}^2 , the relationships between these geometrical functionals are constrained by the geometric inequalities [2, 11, 12, 13, 19, 20, 21, 22] referenced in the second column of Table 2.1. Some geometric inequalities are restricted to convex sets [16], that are not considered in this paper. These inequalities link geometrical functionals by pairs and determine the so-called extremal simply connected compact sets that satisfy the corresponding equalities (Table 2.1, fourth column). Furthermore, they allow to determine morphometrical functionals.

2.3 Morphometrical functionals The morphometrical functionals are invariant under similitude transformations (consequently, they do not depend on the global size of the simply connected compact set) and are defined as ratios between geometrical functionals. In these ratios, the units of the numerator and the denominator are dimensionally homogeneous and the result has therefore no unit. Moreover,

a normalization by a constant value (scalar multiplication) allows to have a ratio that ranges in $[0, 1]$. For each morphometrical functional, the scalar value depends directly on the associated geometric inequality. These morphometrical functionals are referenced in the third column of Table 2.1. These morphometrical functionals are classified according to their concrete meanings: roundness, circularity, diameter constancy and thinness [16].

Table 2.1 synthesizes the geometrical and morphometrical functionals, the geometric inequalities and the extremal 2D analytic simply connected compact sets.

Geometrical functionals	Geometric inequalities	Morphometrical functionals	Extremal sets
r, R	$r \leq R$	r/R	C
ω, R	$\omega \leq 2R$	$\omega/2R$	C
A, R	$A \leq \pi R^2$	$A/\pi R^2$	C
d, R	$d \leq 2R$	$d/2R$	Y
r, d	$2r \leq d$	$2r/d$	C
ω, d	$\omega \leq d$	ω/d	W
A, d	$4A \leq \pi d^2$	$4A/\pi d^2$	C
R, d	$\sqrt{3}R \leq d$	$\sqrt{3}R/d$	Z
r, P	$2\pi r \leq P$	$2\pi r/P$	C
ω, P	$\pi \omega \leq P$	$\pi \omega/P$	W
A, P	$4\pi A \leq P^2$	$4\pi A/P^2$	C
d, P	$2d \leq P$	$2d/P$	L
R, P	$4R \leq P$	$4R/P$	L
r, A	$\pi r^2 \leq A$	$\pi r^2/A$	C
r, ω	$2r \leq \omega$	$2r/\omega$	X

Extremal sets are the sets for which an inequality becomes an equality.

C the disks

W the constant width compact convex sets

L the line segments

X some compact convex sets

Y some simply connected compact sets

Z every compact convex set of diameter d containing an equilateral triangle of side-length d

Table 2.1: Shape functionals for simply connected compact sets. A, P, r, R, ω, d , denote the area, perimeter, radii of the inscribed and circumscribed circles, minimum and maximum Feret diameters [6], respectively.

3 SHAPE DIAGRAMS

From these morphometrical functionals, 2D shape diagrams can be defined. They enable to represent the morphology of any analytic simply connected compact sets in the Euclidean 2D plane from two morphometrical functionals (that is to say from three geometrical functionals because the two denominators use the same geometrical functionals).

3.1 Definition Let be any triplet of the considered six geometrical functionals (A, P, r, R, ω, d) and (M_1, M_2) be some particular morphometrical functionals valued in $[0, 1]^2$ (Table 3.1). A shape diagram \mathcal{D} is represented in the plane domain $[0, 1]^2$ (whose axis coordinates are the morphometrical functionals M_1 and M_2) where any 2D compact set S is mapped onto a point (x, y) . Note that if M_1 or M_2 is in $\{\pi r^2/A, 2r/\omega\}$, the line curves can not be mapped onto a point because they provide null values for A and ω . In other terms, a shape diagram \mathcal{D} is obtained from the following mapping:

$$\mathcal{D} : \begin{cases} \mathcal{K}(\mathbb{E}^2) & \rightarrow [0, 1]^2 \\ S & \mapsto (x, y) \end{cases}$$

where $\mathcal{K}(\mathbb{E}^2)$ denotes the compact sets of the Euclidean 2D plane. Using the morphometrical functionals listed in Table 2.1, twenty-two shape diagrams are defined, and by preserving the notation and indexing used in [16], they are denoted $(\mathcal{D}_k)_{k \in \llbracket 1, 30 \rrbracket \setminus (\llbracket 7, 10 \rrbracket \cup \llbracket 17, 20 \rrbracket)}$, respectively. Some geometric inequalities, and consequently some shape diagrams, are restricted to convex shapes [16], that are not considered in this paper.

Shape diagrams	Axes coordinates	
$\mathcal{D}_1 : (\omega, r, R)$	$x = \omega / 2 R$	$y = r / R$
$\mathcal{D}_2 : (\omega, A, R)$	$x = \omega / 2 R$	$y = A / \pi R^2$
$\mathcal{D}_3 : (r, A, R)$	$x = r / R$	$y = A / \pi R^2$
$\mathcal{D}_4 : (A, d, R)$	$x = A / \pi R^2$	$y = d / 2 R$
$\mathcal{D}_5 : (\omega, d, R)$	$x = \omega / 2 R$	$y = d / 2 R$
$\mathcal{D}_6 : (r, d, R)$	$x = r / R$	$y = d / 2 R$
$\mathcal{D}_{11} : (\omega, r, d)$	$x = \omega / d$	$y = 2 r / d$
$\mathcal{D}_{12} : (\omega, A, d)$	$x = \omega / d$	$y = 4 A / \pi d^2$
$\mathcal{D}_{13} : (r, A, d)$	$x = 2 r / d$	$y = 4 A / \pi d^2$
$\mathcal{D}_{14} : (A, R, d)$	$x = 4 A / \pi d^2$	$y = \sqrt{3} R / d$
$\mathcal{D}_{15} : (\omega, R, d)$	$x = \omega / d$	$y = \sqrt{3} R / d$
$\mathcal{D}_{16} : (r, R, d)$	$x = 2 r / d$	$y = \sqrt{3} R / d$
$\mathcal{D}_{21} : (\omega, r, P)$	$x = \pi \omega / P$	$y = 2 \pi r / P$
$\mathcal{D}_{22} : (\omega, A, P)$	$x = \pi \omega / P$	$y = 4 \pi A / P^2$
$\mathcal{D}_{23} : (r, A, P)$	$x = 2 \pi r / P$	$y = 4 \pi A / P^2$
$\mathcal{D}_{24} : (A, R, P)$	$x = 4 \pi A / P^2$	$y = 4 R / P$
$\mathcal{D}_{25} : (\omega, R, P)$	$x = \pi \omega / P$	$y = 4 R / P$
$\mathcal{D}_{26} : (r, R, P)$	$x = 2 \pi r / P$	$y = 4 R / P$
$\mathcal{D}_{27} : (A, d, P)$	$x = 4 \pi A / P^2$	$y = 2 d / P$
$\mathcal{D}_{28} : (\omega, d, P)$	$x = \pi \omega / P$	$y = 2 d / P$
$\mathcal{D}_{29} : (r, d, P)$	$x = 2 \pi r / P$	$y = 2 d / P$
$\mathcal{D}_{30} : (d, R, P)$	$x = 2 d / P$	$y = 4 R / P$

Table 3.1: Axes coordinates of the twenty-two shape diagrams for 2D simply connected compact sets.

The property stated in [16] proving the non-injectivity and non-surjectivity of the mapping that associates a point in a shape diagram $(\mathcal{D}_k)_{k \in \llbracket 1, 30 \rrbracket \setminus (\llbracket 7, 10 \rrbracket \cup \llbracket 17, 20 \rrbracket)}$ to a

compact convex set in \mathbb{E}^2 , is necessarily truth for the 2D simply connected compact sets. The proof uses the same examples as in [16].

3.2 Complete systems of inequalities In this subsection, only 2D compact convex sets are considered. A system of (two) geometric inequalities associated to a shape diagram is complete if and only if for any range of geometrical functionals values satisfying those conditions, a 2D compact convex set with these geometrical functionals values exists [8, 18]. In other words, such a system is complete if and only if the mapping which associates a 2D analytic compact convex set in \mathbb{E}^2 to a point in a shape diagram $(\mathcal{D}_k)_{k \in \llbracket 1, 30 \rrbracket \setminus (\llbracket 7, 10 \rrbracket \cup \llbracket 17, 20 \rrbracket)}$ can be surjective by restricting the arrival set. For a shape diagram, each of the two associated inequalities determines a part of the convex domain boundary (the domain in which all compact convex sets are mapped). These two inequalities determine the whole boundary of the convex domain if and only if they form a complete system. The compact convex sets mapped onto the boundary points are the extremal compact convex sets of each considered inequality.

For sixteen among the twenty-two shape diagrams $(\mathcal{D}_1, \mathcal{D}_3, \mathcal{D}_4, \mathcal{D}_5, \mathcal{D}_6, \mathcal{D}_{11}, \mathcal{D}_{12}, \mathcal{D}_{14}, \mathcal{D}_{15}, \mathcal{D}_{16}, \mathcal{D}_{22}, \mathcal{D}_{23}, \mathcal{D}_{24}, \mathcal{D}_{26}, \mathcal{D}_{28}, \mathcal{D}_{30})$, the completeness of systems of inequalities has been proved [3, 7, 8, 9, 10, 18]. Figure 4.2 illustrates the convex domain boundary for seven of them.

4 SHAPE DIAGRAMS DISPERSION QUANTIFICATION

4.1 Shape diagrams for simply connected compact sets For the family \mathcal{F}_1^{sc} of nineteen sets (Figure 4.1), the morphometrical functionals are straightforwardly computed. Each simply connected compact set $i \in \llbracket 1, 19 \rrbracket$ is represented by one point denoted $\mathcal{P}_{i,k}$, in each shape diagram \mathcal{D}_k , $k \in \llbracket 1, 30 \rrbracket \setminus (\llbracket 7, 10 \rrbracket \cup \llbracket 17, 20 \rrbracket)$.

These 2D analytic simply connected compact sets are (Figure 4.1):

- line segments;
- "1/2" semi-rings;
- equilateral triangles;
- asterisks-3;
- semi-disks;
- squares;
- asterisks-4;
- disks;
- regular pentagons;
- asterisks-7;
- Reuleaux triangles [5, 15];
- regular hexagons;
- asterisks-8;
- dual Reuleaux triangles;
- regular pentagrams;
- semi-circles;
- dual "Reuleaux" squares;
- regular hexagrams;
- regular crosses: they are symmetrical (center) crosses whose the four branch length and width are equals.

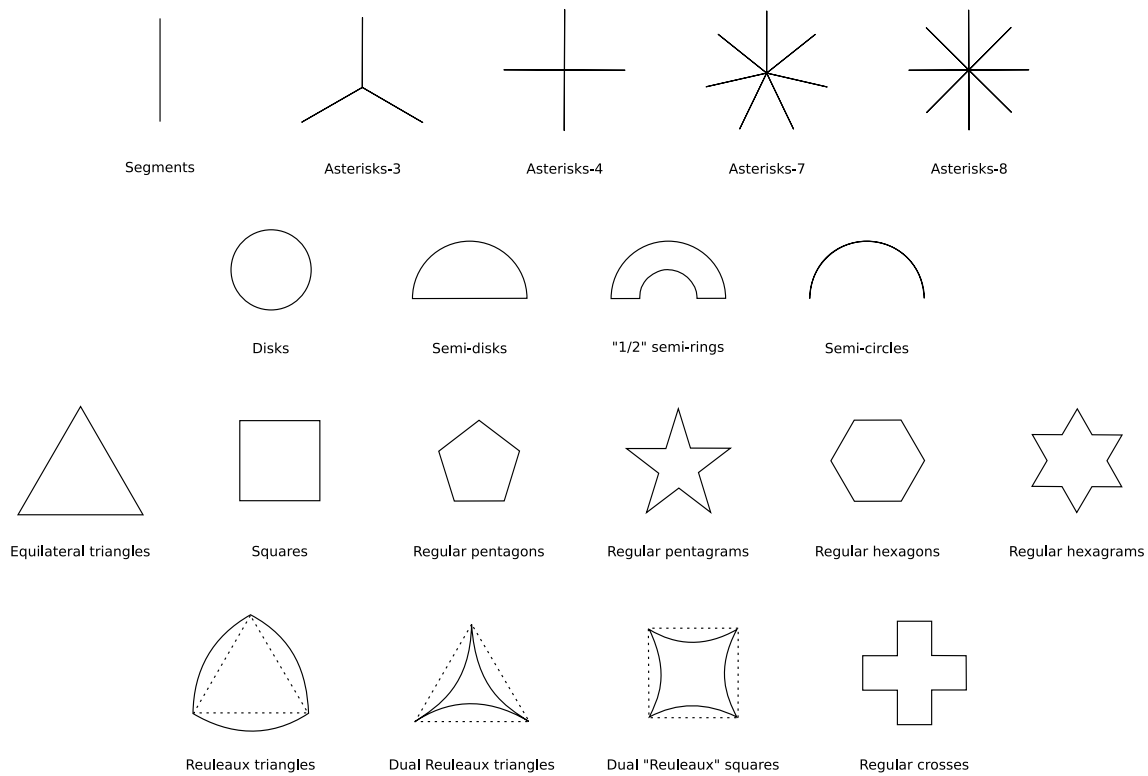


Figure 4.1: Family \mathcal{F}_1^{sc} of 2D analytic simply connected compact sets.

Figure 4.3 illustrates several of these twenty-two shape diagrams, chosen according to the results synthesized in section 6. Remember that the shape diagrams are included in $[0, 1]^2$. For a better visualization of the shapes drawn on a point of abscissa or ordinate equal to 0 or 1, the shape diagrams are illustrated in $[-0.06, 1.04]^2$. Whatever the morphometrical functional, the extremal value 1 is reached for extremal simply connected compact sets. Thus, in each shape diagram, there is at least one simply connected compact set mapped to a point of abscissa or ordinate equal to 1. Moreover, the extremal value 0 is not always reached.

The dispersion of simply connected compact set locations within each shape diagram will be studied after the analysis of similarities between shape diagrams.

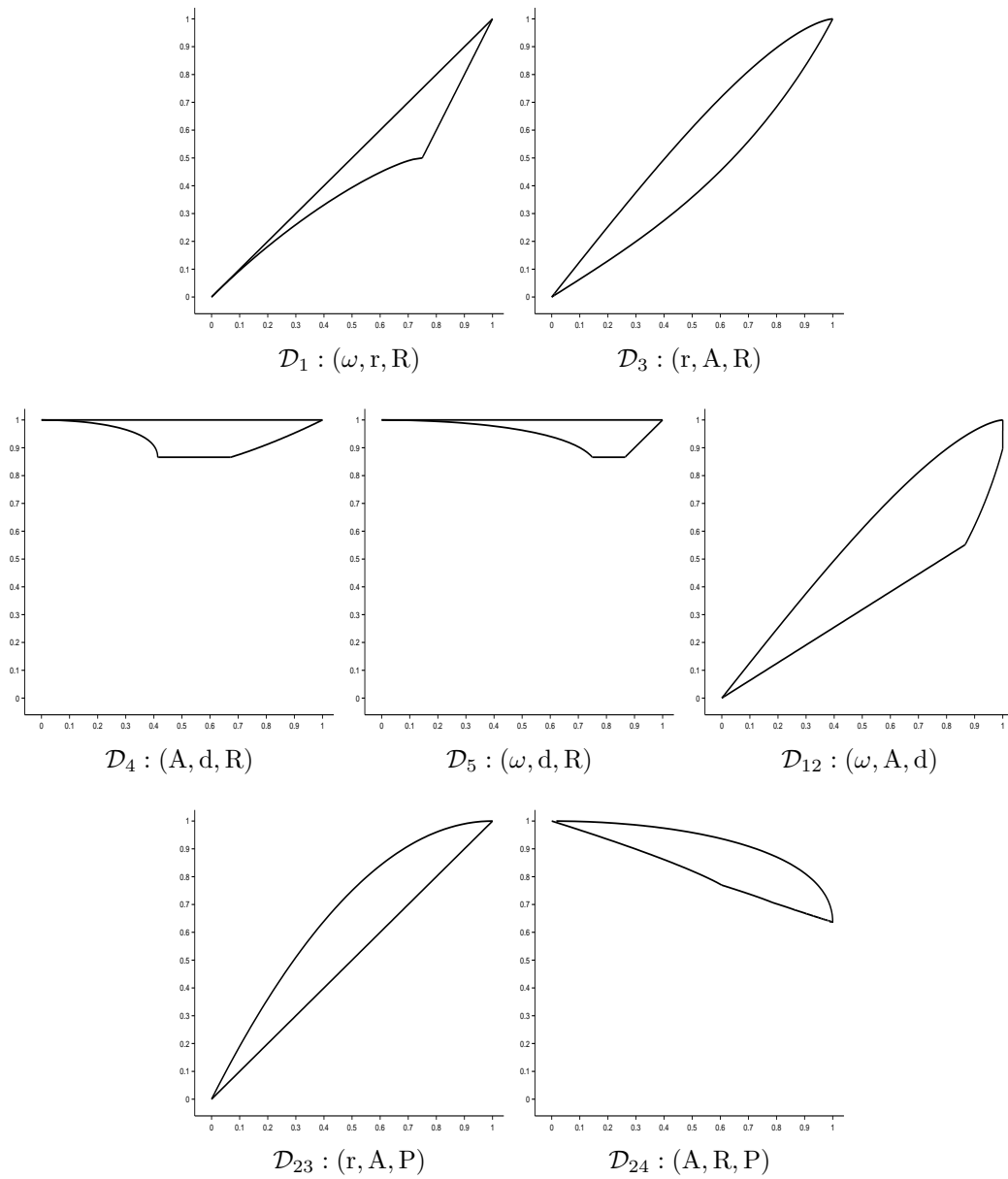


Figure 4.2: Convex domains of seven shape diagrams for which complete systems of inequalities have been established. For a given shape diagram, the bordered region represents the convex domain in which all compact convex sets lay.

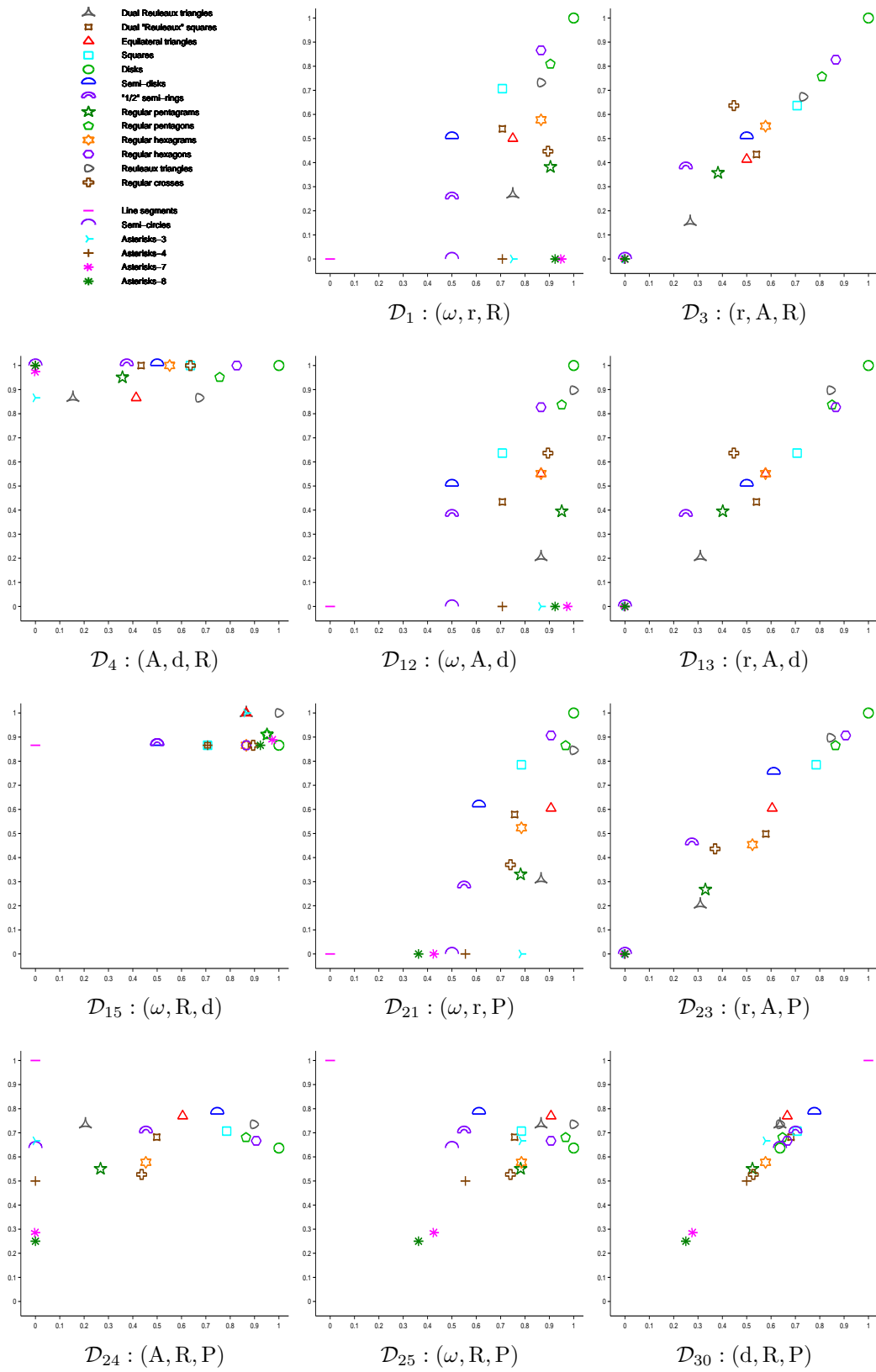


Figure 4.3: Family \mathcal{F}_1^{sc} of analytic simply connected compact sets mapped into eleven shape diagrams (chosen according to the results synthesized in section 6).

4.2 Similarity The fact that $\omega = 2r$ for some compact convex sets implies that shape diagrams (ω, x_1, x_2) are similar to shape diagrams (r, x_1, x_2) where $x_1 \in \{d, R, P, A\}$ and $x_2 \in \{d, R, P\}$, that is to say $\mathcal{D}_2 \sim \mathcal{D}_3$, $\mathcal{D}_5 \sim \mathcal{D}_6$, $\mathcal{D}_{12} \sim \mathcal{D}_{13}$, $\mathcal{D}_{15} \sim \mathcal{D}_{16}$, $\mathcal{D}_{22} \sim \mathcal{D}_{23}$, $\mathcal{D}_{25} \sim \mathcal{D}_{26}$, $\mathcal{D}_{28} \sim \mathcal{D}_{29}$ where \sim denotes a strong similarity between shape diagrams.

In the same way, the fact that $d = 2R$ for some simply connected compact sets implies that:

- shape diagrams (x_1, x_2, R) are similar to shape diagrams (x_1, x_2, d) where $x_1 \in \{\omega, r, A\}$ and $x_2 \in \{r, A, P\}$ ($\mathcal{D}_1 \sim \mathcal{D}_{11}$, $\mathcal{D}_2 \sim \mathcal{D}_{12}$, $\mathcal{D}_3 \sim \mathcal{D}_{13}$);
- shape diagrams (x_1, R, P) are similar to shape diagrams (x_1, d, P) where $x_1 \in \{\omega, r, A\}$ ($\mathcal{D}_{24} \sim \mathcal{D}_{27}$, $\mathcal{D}_{25} \sim \mathcal{D}_{28}$, $\mathcal{D}_{26} \sim \mathcal{D}_{29}$).

An algorithm of hierarchical classification [4] based on distances between shape diagrams allows to justify many of these similarities and to find other ones. Let $k_1, k_2 \in \llbracket 1, 30 \rrbracket \setminus (\llbracket 7, 10 \rrbracket \cup \llbracket 17, 20 \rrbracket)$, the distance between shape diagrams \mathcal{D}_{k_1} and \mathcal{D}_{k_2} , based on the Euclidean distance d^E , is defined by Equation 4.1.

$$(4.1) \quad d^E(\mathcal{D}_{k_1}, \mathcal{D}_{k_2}) = \frac{1}{19} \sum_{i \in \llbracket 1, 19 \rrbracket} d^E(\mathcal{P}_{i, k_1}, \mathcal{P}_{i, k_2})$$

For all $k_1 \in \llbracket 1, 29 \rrbracket \setminus (\llbracket 7, 10 \rrbracket \cup \llbracket 17, 20 \rrbracket)$ and $k_2 \in \llbracket k_1 + 1, 30 \rrbracket \setminus (\llbracket 7, 10 \rrbracket \cup \llbracket 17, 20 \rrbracket)$, the distances $d^E(\mathcal{D}_{k_1}, \mathcal{D}_{k_2})$ are computed. Among them, the minimum distance value gives the best similarity between two shape diagrams. From these two shape diagrams, a mean shape diagram is built. To each step of the algorithm, two shape diagrams are similar up to the distance computed and they are gathered to build a mean shape diagram. The algorithm can be run until all the shape diagrams are gathered. Figure 4.4 shows the first fifteen steps of the hierarchical tree resulting from this algorithm. The remaining steps are not shown because the distance values are too high and do not present an interest in the study of similarities.

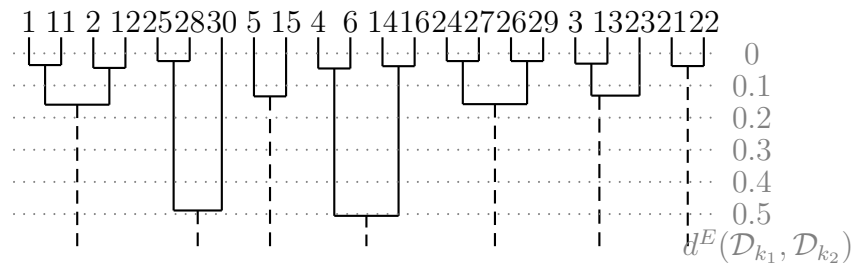


Figure 4.4: The first fifteen steps of an algorithm of hierarchical classification based on distances between the shape diagrams. To each step, two shape diagrams are similar up to the distance value, whose the scale is indicated on the right.

For instance, if the algorithm is stopped before the distance value reaches 0.2, the following classification of shape diagrams is obtained:

- $\mathcal{D}_1, \mathcal{D}_{11}, \mathcal{D}_2, \mathcal{D}_{12}$
- $\mathcal{D}_3, \mathcal{D}_{13}, \mathcal{D}_{23}$
- $\mathcal{D}_4, \mathcal{D}_6$
- $\mathcal{D}_{24}, \mathcal{D}_{27}, \mathcal{D}_{26}, \mathcal{D}_{29}$
- $\mathcal{D}_5, \mathcal{D}_{15}$
- $\mathcal{D}_{14}, \mathcal{D}_{16}$
- $\mathcal{D}_{21}, \mathcal{D}_{22}$
- $\mathcal{D}_{25}, \mathcal{D}_{28}$
- \mathcal{D}_{30}

4.3 Dispersion quantification For each shape diagram, the dispersion of the locations of 2D analytic simply connected compact sets of the family \mathcal{F}_1^{sc} is studied.

The spatial distribution of simply connected compact sets locations in each shape diagram is characterized and quantified from algorithmic geometry using Delaunay's graph (DG) and minimum spanning tree (MST) [1]. Some useful information about the disorder and the neighborhood relationships between sets can be deduced. From each geometrical model, it is possible to compute two values from the edge lengths, denoted μ (average) and σ (standard deviation) for DG or MST. The simple reading of the coordinates in the (μ, σ) -plane enables to determine the type of spatial distribution of the simply connected compact set (regular, random, cluster, ...) [14]. The decrease of μ and the increase of σ characterize the shift from a regular distribution toward random and cluster distributions, respectively.

Figure 4.5 represents both values of parameters of the twenty-two shape diagrams for each model, DG and MST.

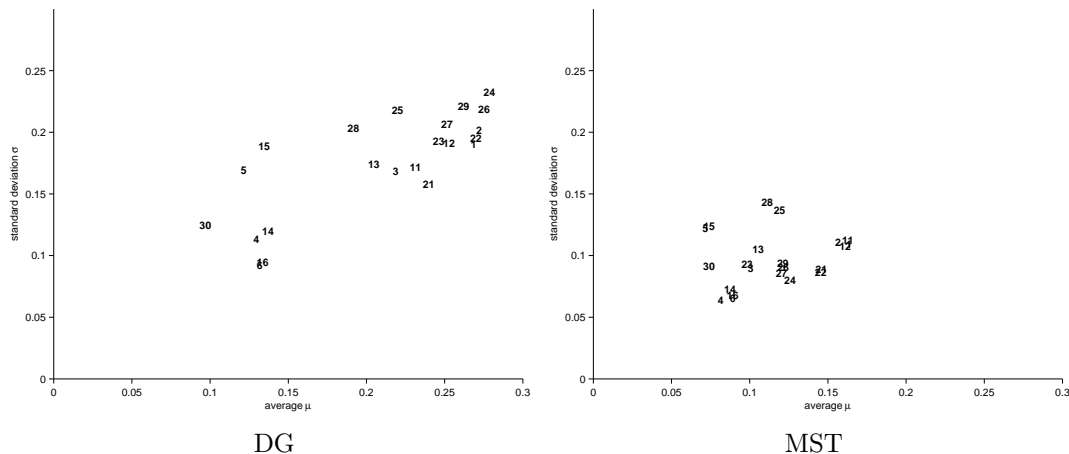


Figure 4.5: Two dispersion quantifications for all shape diagrams applied on the family \mathcal{F}_1^{sc} . For each representation (according to the models DG and MST, respectively), indices $k \in \llbracket 1, 30 \rrbracket \setminus (\llbracket 7, 10 \rrbracket \cup \llbracket 17, 20 \rrbracket)$ of the shape diagrams \mathcal{D}_k are located according to their μ and σ values.

Following the two models, the shape diagrams $\mathcal{D}_4, \mathcal{D}_5, \mathcal{D}_6, \mathcal{D}_{14}, \mathcal{D}_{15}, \mathcal{D}_{16}$ and \mathcal{D}_{30} have a low average μ . In these shape diagrams, the simply connected compact sets are located within a restricted domain in $[0, 1]^2$. Their shape discrimination is not strong, especially for \mathcal{D}_5 and \mathcal{D}_{15} that have a higher standard deviation σ , which is translated visually by several sets at the same locations.

The shape diagrams $\mathcal{D}_1, \mathcal{D}_2, \mathcal{D}_{11}, \mathcal{D}_{12}, \mathcal{D}_{21}, \mathcal{D}_{22}, \mathcal{D}_{24}, \mathcal{D}_{26}, \mathcal{D}_{27}$ and \mathcal{D}_{29} have the highest averages. In these shape diagrams, the simply connected compact sets are located within a large domain in $[0, 1]^2$ and are well spaced from each other.

Finally, these statements are in agreement with those obtained for the similarities between shape diagrams.

A shape diagram with a strong dispersion (both high μ and σ values), for both DG and MST, guarantees a strong discrimination of shapes: the simply connected compact sets are located within a large domain in $[0, 1]^2$ and are well spaced from each other. However, remember that $d = 2R$ and $\omega = 2r$ for some simply connected

compact sets. This explains that some simply connected compact sets of the family \mathcal{F}_1^{sc} are mapped onto a point on a line for some shape diagrams, namely:

- diagonal line from $(0, 0)$ to $(1, 1)$ on shape diagrams (x_1, x_2, x_3) where $(x_1, x_2) \in \{(\omega, r), (d, R)\}$ and $x_3 \in \{A, R, d, P\}$ ($\mathcal{D}_1, \mathcal{D}_{11}, \mathcal{D}_{21}, \mathcal{D}_{30}$)
- horizontal line from $(0, 1)$ to $(1, 1)$ on shape diagrams (x_1, d, R) where $x_1 \in \{\omega, r, P, A\}$ ($\mathcal{D}_4, \mathcal{D}_5, \mathcal{D}_6$)
- horizontal line from $(0, \sqrt{3}/2)$ to $(1, \sqrt{3}/2)$ on shape diagrams (x_1, R, d) where $x_1 \in \{\omega, r, P, A\}$ ($\mathcal{D}_{14}, \mathcal{D}_{15}, \mathcal{D}_{16}$)

For a shape diagram, the fact that some simply connected compact sets are mapped onto a point on a line does not yield to allow a strong discrimination of the simply connected compact sets as quantified and illustrated in Figure 4.5.

Following this quantification, the shape diagrams $\mathcal{D}_{24}, \mathcal{D}_{25}, \mathcal{D}_{26}, \mathcal{D}_{27}, \mathcal{D}_{28}$ and \mathcal{D}_{29} , have a strong dispersion. During the study restricted to convex sets [16], they appear more moderate. The other shape diagrams have dispersions quite similar to those obtained with the convex sets.

5 SHAPE DIAGRAMS OVERLAPPING QUANTIFICATION

5.1 Shape diagrams for simply connected compact sets with one degree of freedom

Let two 2D analytic simply connected compact sets of the family \mathcal{F}_1^{sc} , and the simply connected compact set class allowing to switch from one to the other using one degree of freedom. For example, the semi-circle goes to the semi-disk through semi-rings whose the cavity radius decreases. Therefore, several classes of "simply connected compact sets with one degree of freedom" could be defined. Thus, a curve denoted $\mathcal{C}_{i,k}$ from each simply connected compact set class C_i is created in each shape diagram \mathcal{D}_k , $k \in \llbracket 1, 30 \rrbracket \setminus (\llbracket 7, 10 \rrbracket \cup \llbracket 17, 20 \rrbracket)$. This process is used for some pairs of simply connected compact sets of the family \mathcal{F}_1^{sc} . The tendency of various curves are observed.

These analytic simply connected compact sets verify shape properties which are preserved only under similitude transformations and under the variation of one parameter $t \in \mathbb{R}$. For example, the cavity radius of semi-rings varies between 0 and the radius of the semi-disk. In other terms, the degree of freedom is the parameter $t \in \mathbb{R}$.

Nineteen analytic simply connected compact set classes, gathered in three families, are considered:

- family $\mathcal{F}_{2,1}^{sc} \supseteq \{C_i\}_{i \in \llbracket 1,4 \rrbracket}$: four classes of simply connected compact sets with one symmetrical axis (Figure 5.1),
- family $\mathcal{F}_{2,2}^{sc} \supseteq \{C_i\}_{i \in \{6,8,10,12,14,16,18,19\}}$: eight classes of simply connected compact sets with an even number of symmetrical axis (Figure 5.2),
- family $\mathcal{F}_{2,3}^{sc} \supseteq \{C_i\}_{i \in \{5,7,9,11,13,15,17\}}$: seven classes of simply connected compact sets with an odd number strictly greater to 1 of symmetrical axis (Figure 5.3).

There are:

- Family $\mathcal{F}_{2,1}^{sc}$:
 C_1 - Semi-rings: They are the complementary sets of a semi-disk in a larger semi-disk. The ratio between the radius of the small and the large semi-disks varies in $[0, 1]$. When it reaches the lower and upper bounds, the semi-ring becomes a semi-disk and a semi-circle, respectively.

C_2 - Semi-disks minus ungula: They are the complementary sets of an ungula [16] in a semi-disk. The ratio between the height of the ungula and the radius of the semi-disk varies in $[0, 1]$. When it reaches the lower and upper bounds, the semi-disk minus ungula becomes a semi-disk and a semi-circle, respectively.

C_3 - Semi-disks minus semi-symmetrical disks with two peaks: They are the complementary sets of a semi-symmetrical disk with two peaks [16] in a semi-disk. The ratio between the height of the semi-symmetrical disk with two peaks and the radius of the semi-disk varies in $[0, 1]$. When it reaches the lower and upper bounds, the semi-disk minus semi-symmetrical disk with two peaks becomes a semi-disk and a semi-circle, respectively.

C_4 - Arrows: They are the complementary sets of an isosceles triangle in an equilateral triangle. The ratio between the height of the isosceles and the equilateral triangles varies in $[0, 1]$. When it reaches the lower and upper bounds, the arrow becomes an equilateral triangle and a shape with two line segments forming an angle whose the value is equal to $\pi/3$, respectively.

- Family $\mathcal{F}_{2,2}^{sc}$:

C_6 - Dual "Yamanouti" squares: They are defined in a similar way as the "Yamanouti" squares [16]. The extremal simply connected compact sets are the square and the dual "Reuleaux" square.

C_8 - Four-stars: the filiformity coefficient varies between 0 ($A = 0$) and 1 (square).

C_{10} - Six-stars: the filiformity coefficient varies between 0 ($A = 0$) and 1 (regular hexagon).

C_{12} - Eight-stars: the filiformity coefficient varies between 0 ($A = 0$) and 1 (regular octagon, not illustrated here).

C_{14} - Even-stars, minimal filiformity: Their area value is null. They are asterisks with a branch even number.

C_{16} - Regular even polygrams: They are regular polygrams (the filiformity coefficient is "perfect", involving parallelism between the edges) with a positive even edges number. In the shape diagrams, the real positions of these sets do not describe a curve because it is not continuous (the edge number is necessarily an integer) but they are along a curve, and this is drawn.

C_{18} - Even-stars, maximal filiformity: They are regular even polygons [16].

C_{19} - Crosses: They are symmetrical (center) crosses whose the four branch length varies in $[0, +\infty[$. When this length value reaches the lower bound, the resulting simply connected compact set becomes a square. When it tends to infinity, the resulting simply connected compact set tends to the asterisk-4.

- Family $\mathcal{F}_{2,3}^{sc}$:

C_5 - Dual Yamanouti triangles: They are defined in a similar way as the Yamanouti triangles [23]. The extremal simply connected compact sets are the equilateral triangle and the dual Reuleaux triangle.

C_7 - Three-stars: the filiformity coefficient varies between 0 ($A = 0$) and 1 (equilateral triangle).

C_9 - Five-stars: the filiformity coefficient varies between 0 ($A = 0$) and 1 (regular pentagon).

C_{11} - Seven-stars: the filiformity coefficient varies between 0 ($A = 0$) and 1 (regular heptagon, not illustrated here).

C_{13} - Odd-stars, minimal filiformity: Their area value is null. They are asterisks with a branch odd number.

C_{15} - Regular odd polygrams: They are regular polygrams (the filiformity coefficient is "perfect", involving parallelism between the edges) with a positive odd edges number. In the shape diagrams, the real positions of these sets do not describe a curve because it is not continuous (the edge number is necessarily an integer) but they are along a curve, and this is drawn.

C_{17} - Odd-stars, maximal filiformity: They are regular odd polygons [16].

For the simply connected compact sets of each class, the morphometrical functionals are computed. In each shape diagram \mathcal{D}_k , $k \in \llbracket 1, 30 \rrbracket \setminus (\llbracket 7, 10 \rrbracket \cup \llbracket 17, 20 \rrbracket)$, a simply connected compact set class $i \in \llbracket 1, 19 \rrbracket$ is represented by a parametric curve $\mathcal{C}_{i,k}(t)$ since the class is infinite and bounded by the two extremal sets. For the considered simply connected compact set classes, the extremal simply connected compact sets are sets that would be able to be in the family \mathcal{F}_1^{sc} (Figure 4.1). For example, up to a similitude transformation, an infinite class of semi-rings exists, from the semi-circle to the semi-disk.

Figures 5.4, 5.5 and 5.6 illustrate some of these shape diagrams, chosen according to the results synthetized in section 6.

5.2 Overlapping quantification An overlapping of curves is visible in some shape diagrams. Its quantification is based on a discretization of the spatial domain $[0, 1]^2$ of shape diagrams, depending on the discretization level $n \in \mathbb{N}^*$ [16].

Equation 5.1 quantifies (by a measurement ranging between 0 and 1) the overlapping of all curves for each shape diagram \mathcal{D}_k , $k \in \llbracket 1, 30 \rrbracket \setminus (\llbracket 7, 10 \rrbracket \cup \llbracket 17, 20 \rrbracket)$. A high (resp. low) value for this ratio means a strong (resp. weak) overlapping. When the computation is done for various discretization parameter n values, not only the curves overlapping is considered but also the curves proximity (small n value).

$$(5.1) \quad \text{Overlapping}_n(\mathcal{D}_k) = 1 - \frac{\sum_{(x,y) \in \llbracket 0, n \rrbracket^2} D_k^{max}(x, y)}{\sum_{(x,y) \in \llbracket 0, n \rrbracket^2} D_k^{sum}(x, y)}$$

where $D_k^{max} : \llbracket 0, n \rrbracket^2 \rightarrow \{0, 1\}$ and $D_k^{sum} : \llbracket 0, n \rrbracket^2 \rightarrow \mathbb{N}$ are defined $\forall (x, y) \in \llbracket 0, n \rrbracket^2$ by:

$$D_k^{max}(x, y) = \max_{i \in \llbracket 1, 23 \rrbracket} C_{i,k}(x, y)$$

$$D_k^{sum}(x, y) = \sum_{i \in \llbracket 1, 23 \rrbracket} C_{i,k}(x, y)$$

$C_{i,k}$ denoted the discretization of the curve $\mathcal{C}_{i,k}$ [16].

Figure 5.7 illustrates the discretized shape diagrams ($n = 100$) with overlapping intensities, and Figure 5.8 shows the quantification of curves overlapping (representing the simply connected compact set classes) for some shape diagrams, according to the n values 100 and 1000.

Several informations can be extracted from these graphs:

- The graphs representing the 2D analytic simply connected compact set classes of the family $\mathcal{F}_{2,1}^{sc}$ show a strong overlap (from $n = 1000$) for the shape diagrams $\mathcal{D}_1, \mathcal{D}_2, \mathcal{D}_4, \mathcal{D}_5, \mathcal{D}_6, \mathcal{D}_{11}, \mathcal{D}_{12}, \mathcal{D}_{14}, \mathcal{D}_{15}, \mathcal{D}_{16}, \mathcal{D}_{25}, \mathcal{D}_{28}$ and \mathcal{D}_{30} .

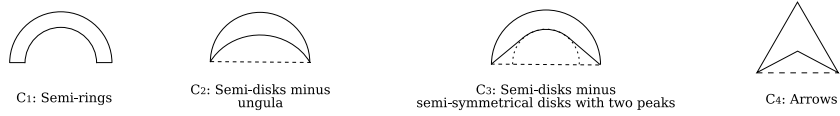


Figure 5.1: Family $\mathcal{F}_{2,1}^{sc}$ of 2D analytic simply connected compact sets with one degree of freedom and one symmetrical axis.

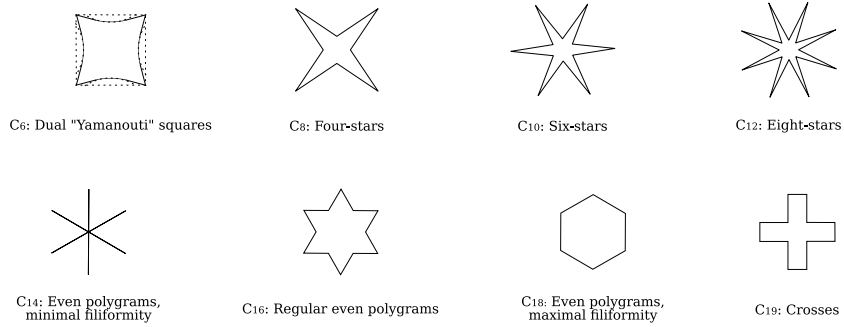


Figure 5.2: Family $\mathcal{F}_{2,2}^{sc}$ of 2D analytic simply connected compact sets with one degree of freedom and an even number of symmetrical axes.

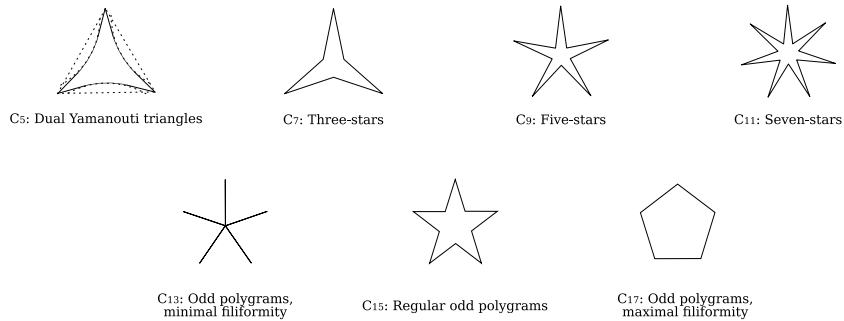


Figure 5.3: Family $\mathcal{F}_{2,3}^{sc}$ of 2D analytic simply connected compact sets with one degree of freedom and an odd number (strictly greater to 1) of symmetrical axes.

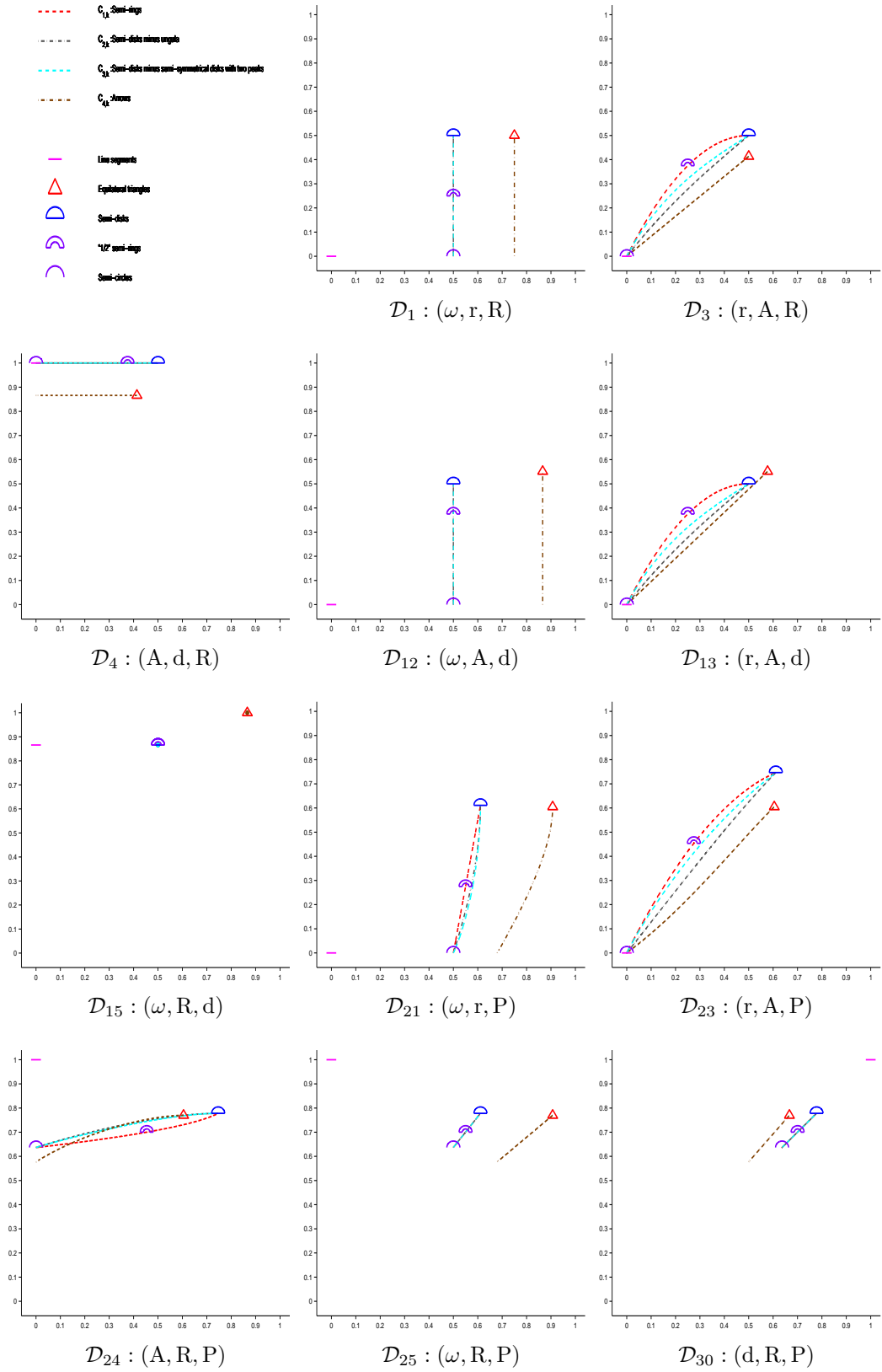


Figure 5.4: Family $\mathcal{F}_{2.1}^{sc}$ of analytic simply connected compact sets with one degree of freedom and one symmetrical axis mapped into eleven shape diagrams (chosen according to the results synthesized in section 6).

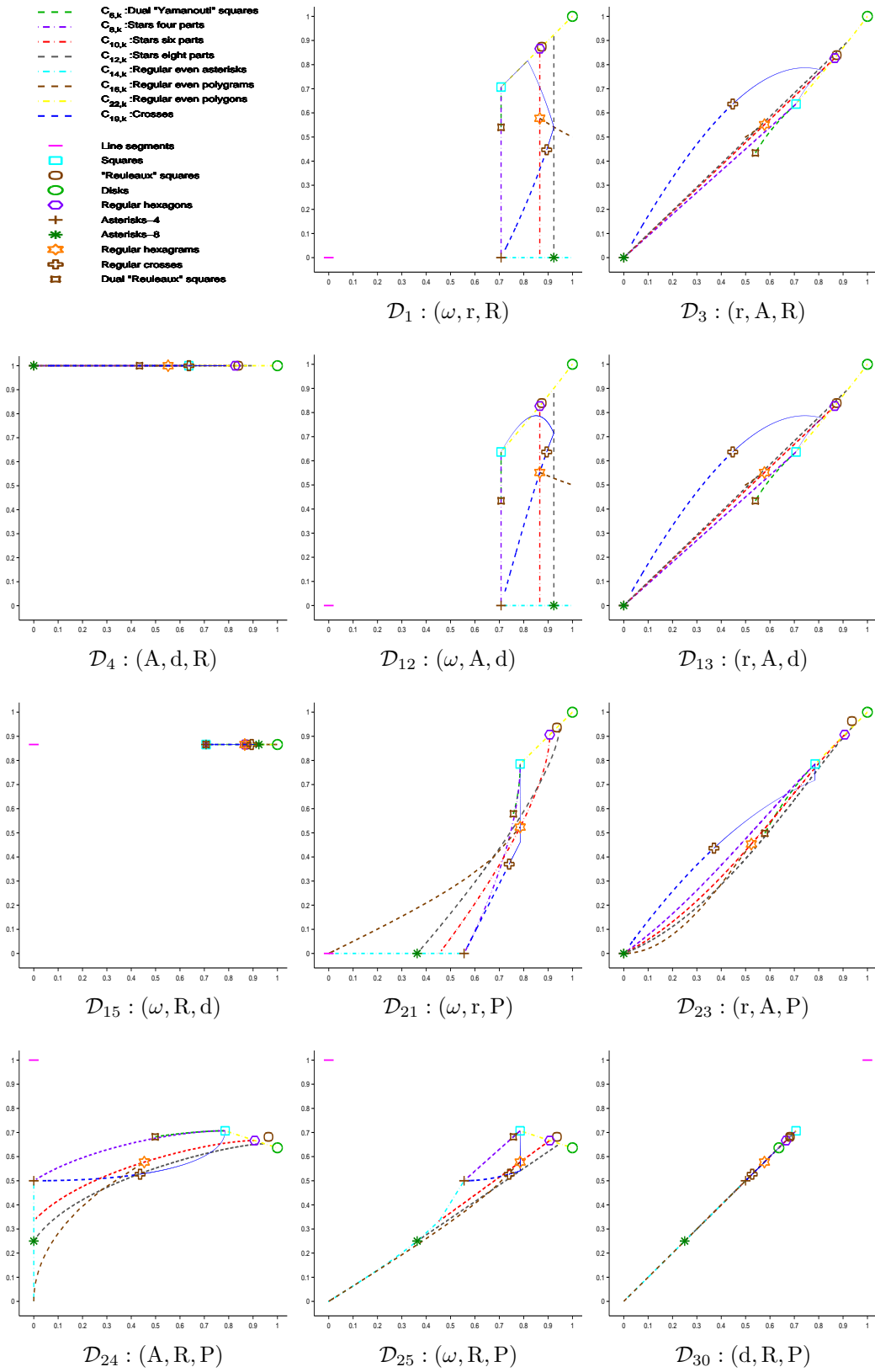


Figure 5.5: Family $\mathcal{F}_{2,2}^{sc}$ of analytic simply connected compact sets with one degree of freedom and an odd number of symmetrical axes mapped into eleven shape diagrams (chosen according to the results synthesized in section 6).

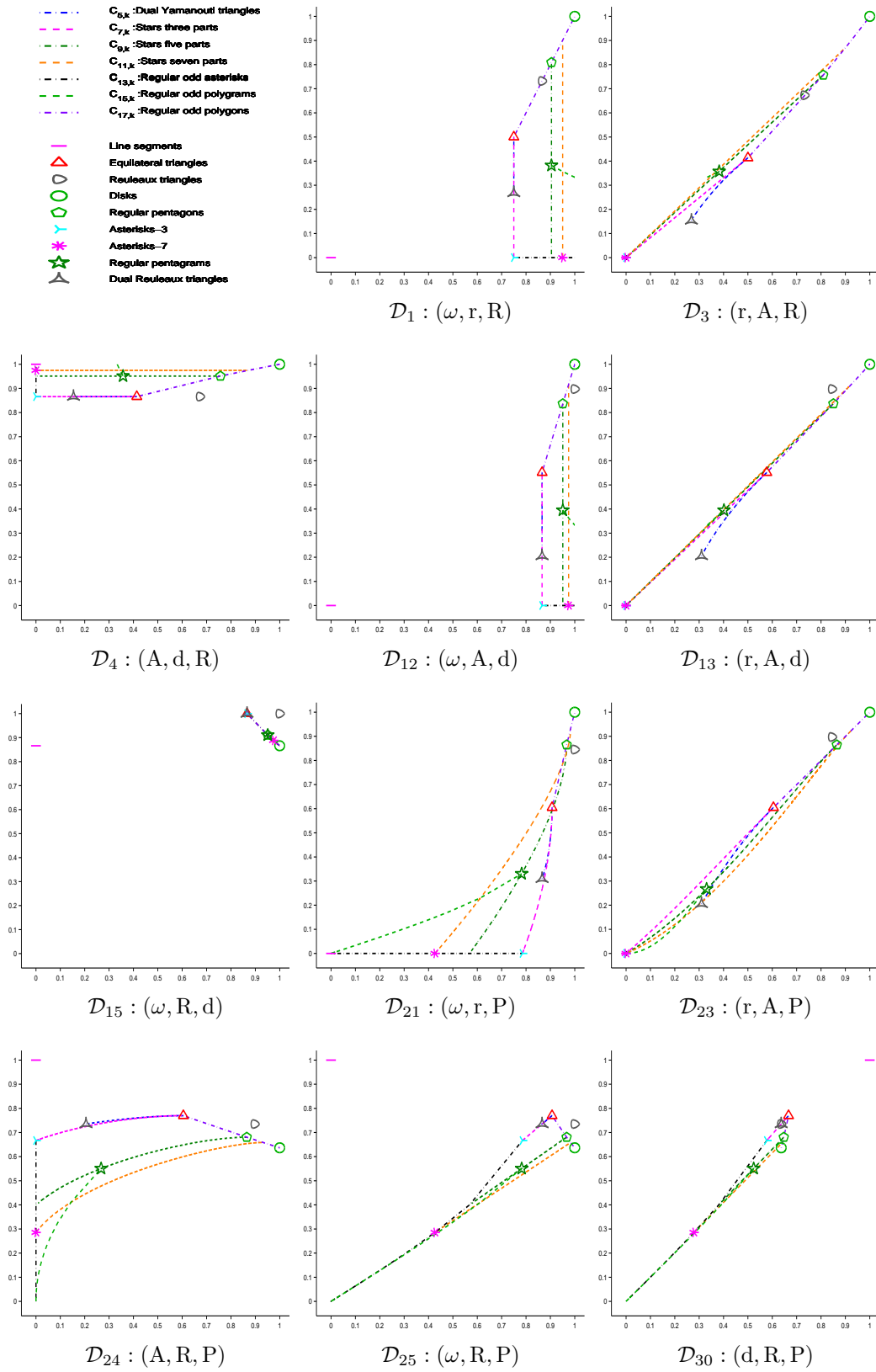


Figure 5.6: Family $\mathcal{F}_{2,3}^{sc}$ of analytic simply connected compact sets with one degree of freedom and an even number strictly greater to 1 of symmetrical axes mapped into eleven shape diagrams (chosen according to the results synthesized in section 6).

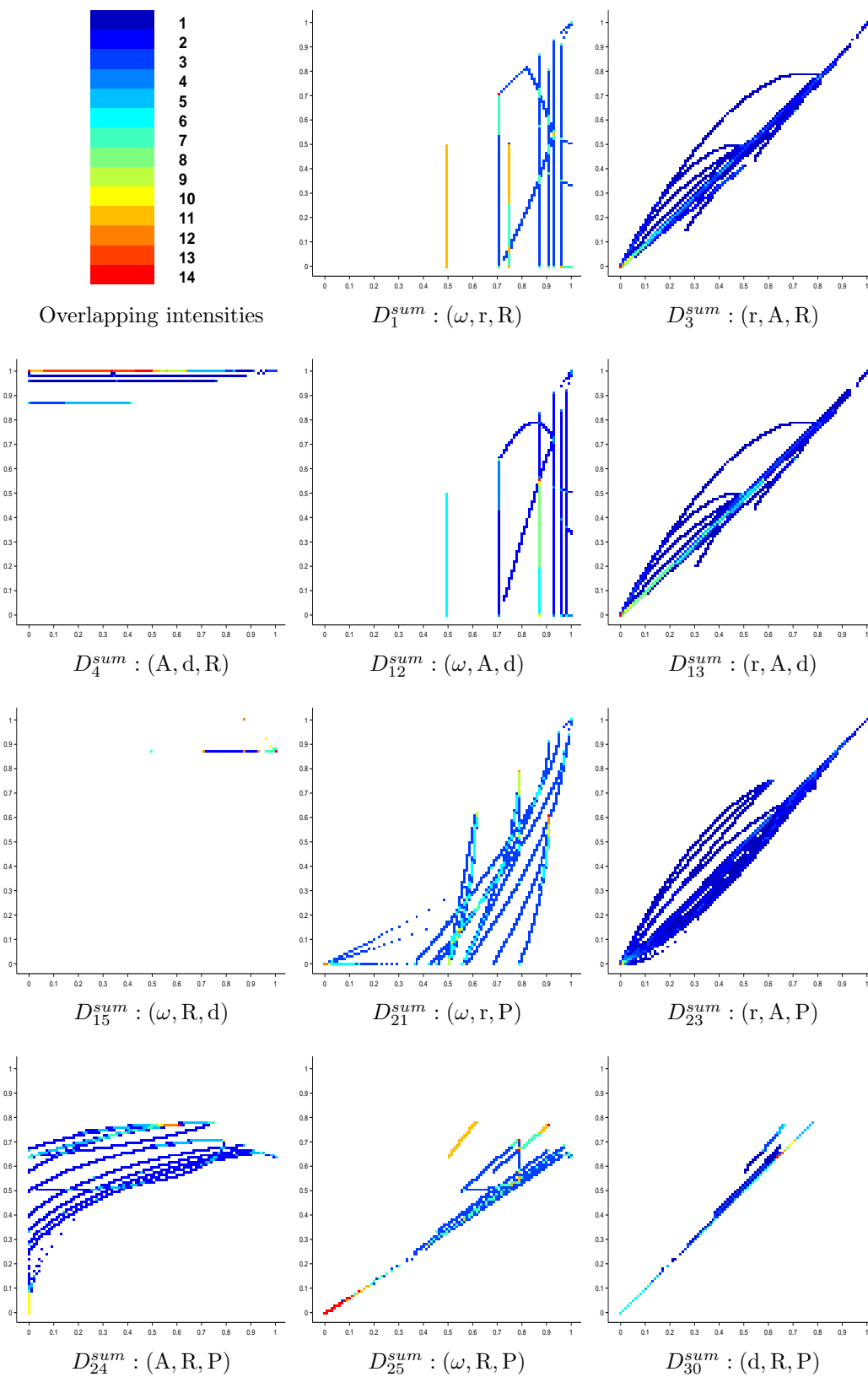
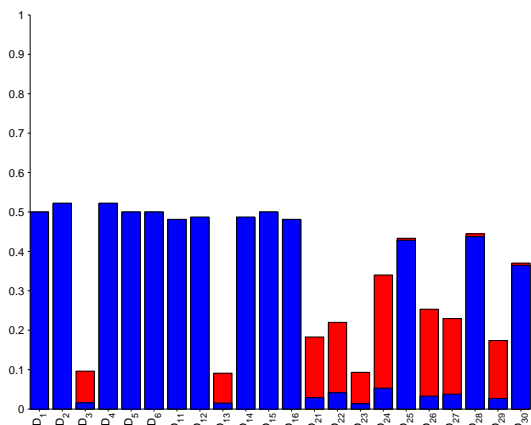
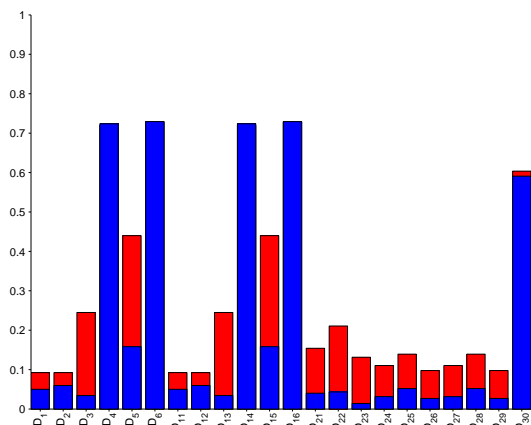


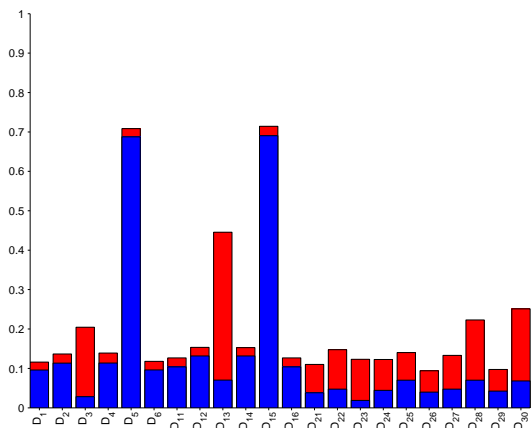
Figure 5.7: "Intensity" discretized shape diagram D_k^{sum} ($n = 100$) with the nineteen curves representing the simply connected compact set classes with one degree of freedom.



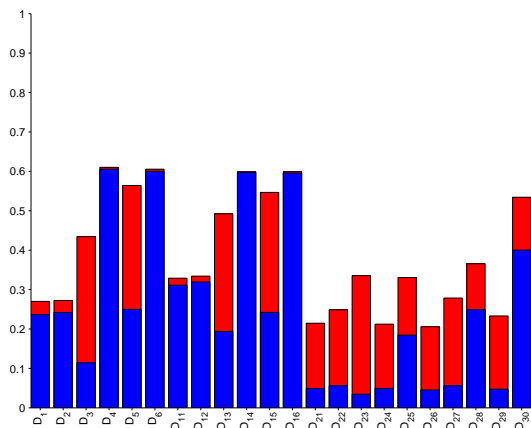
Overlapping quantification for the family $\mathcal{F}_{2,1}^{sc}$ of simply connected compact sets with one degree of freedom and one symmetrical axis.



Overlapping quantification for the family $\mathcal{F}_{2,2}^{sc}$ of simply connected compact sets with one degree of freedom and an even number of symmetrical axes.



Overlapping quantification for the family $\mathcal{F}_{2,3}^{sc}$ of simply connected compact sets with one degree of freedom and an odd number strictly greater to 1 of symmetrical axes.



Overlapping quantification for the nineteen classes of simply connected compact sets with one degree of freedom.

Figure 5.8: Overlapping quantification for the twenty-two shape diagrams \mathcal{D}_k , $k \in \llbracket 1, 30 \rrbracket \setminus (\llbracket 7, 10 \rrbracket \cup \llbracket 17, 20 \rrbracket)$, with $n = 100$ in red, and $n = 1000$ in blue.

- The graphs representing the 2D analytic simply connected compact set classes of the family $\mathcal{F}_{2,2}^{sc}$ show a strong overlap (from $n = 1000$) in the shape diagrams \mathcal{D}_4 , \mathcal{D}_6 , \mathcal{D}_{14} , \mathcal{D}_{16} and \mathcal{D}_{30} . They are close to each other (strong overlap from $n = 100$) in the shape diagrams \mathcal{D}_5 and \mathcal{D}_{15} .
- The graphs representing the 2D analytic simply connected compact set classes of the family $\mathcal{F}_{2,3}^{sc}$ show a strong overlap (from $n = 1000$) in the shape diagrams \mathcal{D}_5 and \mathcal{D}_{15} . They are close to each other (strong overlap from $n = 100$) in the shape diagram \mathcal{D}_{13} .

Generally speaking, the results obtained with this quantification are quite different from those obtained during the study restricted to convex sets [16].

6 SYNTHESIS

To obtain a strong discrimination of 2D analytic simply connected compact sets, it is necessary to have both a strong dispersion and a weak overlapping.

- The shape diagrams \mathcal{D}_5 and \mathcal{D}_{15} are excluded due to their weak dispersion and overlapping results, whatever the considered simply connected compact sets.
- In the shape diagrams \mathcal{D}_4 , \mathcal{D}_6 , \mathcal{D}_{14} , \mathcal{D}_{16} and \mathcal{D}_{30} , only the family $\mathcal{F}_{2,3}^{sc}$ shows a weak overlapping. Furthermore, their dispersion quantification is weak.
- In the shape diagrams \mathcal{D}_{25} and \mathcal{D}_{28} , the family $\mathcal{F}_{2,1}^{sc}$ shows a strong overlapping. Furthermore, their dispersion quantification is moderate.
- In the shape diagrams \mathcal{D}_1 , \mathcal{D}_2 , \mathcal{D}_{11} and \mathcal{D}_{12} , the family $\mathcal{F}_{2,1}^{sc}$ shows a strong overlapping. Furthermore, their dispersion quantification is strong.
- In addition to their strong dispersion, the shape diagrams \mathcal{D}_3 , \mathcal{D}_{13} , \mathcal{D}_{21} , \mathcal{D}_{22} , \mathcal{D}_{23} , \mathcal{D}_{24} , \mathcal{D}_{26} , \mathcal{D}_{27} and \mathcal{D}_{29} provide a weak overlapping of the simply connected compact set classes considered in this paper.

Furthermore, among the shape diagrams \mathcal{D}_3 , \mathcal{D}_{13} , \mathcal{D}_{21} , \mathcal{D}_{22} , \mathcal{D}_{23} , \mathcal{D}_{24} , \mathcal{D}_{26} , \mathcal{D}_{27} and \mathcal{D}_{29} that obtain the best results for dispersion and overlapping quantifications, only \mathcal{D}_3 , \mathcal{D}_{22} , \mathcal{D}_{23} , \mathcal{D}_{24} and \mathcal{D}_{26} are based on known complete systems of inequalities. Observing in details the representation of quantifications for these five shape diagrams, \mathcal{D}_{24} is retained for shape discrimination of analytic simply connected compact sets.

This analysis is summarized in Table 6.1.

	Complete system of inequalities	Non-complete system of inequalities
Strong discrimination	$\boxed{\mathcal{D}_3}$, \mathcal{D}_{22} , $\boxed{\mathcal{D}_{23}}$, $\boxed{\mathcal{D}_{24}}$, \mathcal{D}_{26}	$\boxed{\mathcal{D}_{13}}$, $\boxed{\mathcal{D}_{21}}$, \mathcal{D}_{27} , \mathcal{D}_{29}
Moderate discrimination	$\boxed{\mathcal{D}_1}$, \mathcal{D}_{11} , $\boxed{\mathcal{D}_{12}}$, \mathcal{D}_{28}	\mathcal{D}_2 , $\boxed{\mathcal{D}_{25}}$
Weak discrimination	$\boxed{\mathcal{D}_4}$, \mathcal{D}_5 , \mathcal{D}_6 , \mathcal{D}_{14} , $\boxed{\mathcal{D}_{15}}$, \mathcal{D}_{16} , $\boxed{\mathcal{D}_{30}}$	

Table 6.1: Shape diagrams classification according to their quality of shape discrimination of analytic simply connected compact sets and according to the completeness of associated systems of inequalities.

In this paper, only some shape diagrams have been illustrated. The choice was based on the results of shape discrimination (dispersion and overlapping studies) and on the results of similarities between shape diagrams (subsection 4.2). The aim

was to illustrate dissimilar shape diagrams with different qualities of shape discrimination, and shape diagrams with different completeness of associated systems of inequalities. The framed shape diagrams of Table 6.1 are those illustrated throughout this paper.

7 CONCLUSION

This paper has dealt with shape diagrams of 2D non-empty analytic simply connected compact sets built from six geometrical functionals: the area, the perimeter, the radii of the inscribed and circumscribed circles, and the minimum and maximum Feret diameters. Each such a set is represented by a point within a shape diagram whose coordinates are morphometrical functionals defined as normalized ratios of geometrical functionals. From existing morphometrical functionals for these sets, twenty-two shape diagrams can be built. A detailed comparative study has been performed in order to analyze the representation relevance and discrimination power of these shape diagrams. It is based on the dispersion and overlapping quantifications from simply connected compact set locations in diagrams. Among all the shape diagrams, nine present a strong shape discrimination of sets, five are based on complete system of inequalities. Among these five diagrams, the shape diagram $\mathcal{D}_{24} : (A, R, P)$ is retained for its representation relevance and discrimination power.

This paper reports the second part of a general comparative study of shape diagrams. The focus was placed on analytic simply connected compact sets. The first part [16] was restricted to the analytic compact convex sets. The main difference between the study of shape diagrams for the simply connected compact sets and those for the compact convex sets lies in the fact that some are not defined in the simply connected case. Moreover in this case, if the shape diagram is defined, the zone gathering the sets locations is necessarily larger in the simply connected case. The third part [17] of the comparative study is published in a following paper. It focuses on convexity discrimination for analytic and discretized simply connected compact sets.

REFERENCES

- [1] J.D. Boissonnat and M. Yvinec. *Algorithmic geometry*. Cambridge University Press (1998).
- [2] T. Bonnesen and W. Fenchel. *Theorie der konvexen körper*. Springer-Verlag, Berlin (1934, 1974); Chelsea, New-York (1948).
- [3] K. Böröczky Jr., M.A. Hernández Cifre and G. Salinas. Optimizing area and perimeter of convex sets for fixed circumradius and inradius. *Monatshefte für Mathematik*. **138**: 95-110 (2003).
- [4] E. Diday. Croisements, ordres et ultramétriques. *Mathématiques et Sciences humaines*. **83**: 31-54 (1983).
- [5] H.G. Eggleston. A proof of Blaschke's theorem on the Reuleaux triangle. *Quarterly Journal of Mathematics, Oxford* **3(2)**: 296-297 (1952).
- [6] L.R. Feret. La grosseur des grains des matières pulvérulentes. *Premières Communications de la Nouvelle Association Internationale pour l'Essai des Matériaux. Groupe D*: 428-436 Zürich (1930).
- [7] M.A. Hernández Cifre. Is there a planar convex set with given width, diameter, and inradius ? *American Mathematical Monthly*. **107**: 893-900 (2000).

- [8] M.A. Hernández Cifre and S. Segura Gomis. The missing boundaries of the Santaló diagrams for the cases (d, ω, R) and (ω, R, r) . *Discrete and Computational Geometry*. **23**: 381-388 (2000).
- [9] M.A. Hernández Cifre, G. Salinas and S. Segura Gomis. Complete Systems of Inequalities. *Journal of Inequalities in Pure and Applied Mathematics*. **2(1-10)**: 1-12 (2001).
- [10] M.A. Hernández Cifre. Optimizing the perimeter and the area of convex sets with fixed diameter and circumradius. *Archiv der Mathematik*. **79**: 147-157 (2002).
- [11] P.W. Hillock and P.R. Scott. Inequalities for lattice constrained planar convex sets. *Journal of Inequalities in Pure and Applied Mathematics*. **3(2-23)**: 1-10 (2002).
- [12] R. Osserman. The isoperimetric inequality. *Bulletin of the American Mathematical Society* **84**: 1182-1238 (1978).
- [13] R. Osserman. Bonnesen style isoperimetric inequalities. *American Mathematical Monthly*. **86**: 1-29 (1979).
- [14] B.N. Raby, M. Polette, C. Gilles, C. Clavel, K. Strumane, M. Matos, J.M. Zahm, F. Van Roy, N. Bonnet and P. Birembaut. Quantitative cell dispersion analysis: new test to measure tumor cell aggressiveness. *International Union Against Cancer*. **93**: 644-652 (2001).
- [15] F. Reuleaux. *The Kinematics of Machinery: Outlines of a Theory of Machines*. German original (1875). Translated by A. Kennedy, MacMillan and Co., London (1876). Reprinted by Dover, New-York (1963).
- [16] S. Rivollier, J. Debayle and J.C. Pinoli. Shape diagrams for 2D compact sets - Part I: analytic convex sets. *Australian Journal of Mathematical Analysis and Applications*. **7(2-3)**: 1-27 (2010).
- [17] S. Rivollier, J. Debayle and J.C. Pinoli. Shape diagrams for 2D compact sets - Part III: convexity discrimination for analytic and discretized simply connected sets. *Australian Journal of Mathematical Analysis and Applications*. **7(2-5)**: 1-18 (2010).
- [18] L.A. Santaló. Sobre los sistemas completos de desigualdades entre tres elementos de una figura convexa plana. *Math. Notae*. **17**: 82-104 (1961).
- [19] P.R. Scott. A family of inequalities for convex sets. *Bulletin of the Australian Mathematical Society* **20**: 237-245 (1979).
- [20] P.R. Scott and P.W. Awyong. Inequalities for convex sets. *Journal of Inequalities in Pure and Applied Mathematics*. **1(1-6)**: 1-6 (2000).
- [21] A. Siegel. An isoperimetric theorem in plane geometry. *Discrete and Computational Geometry*. **29(2)**: 239-255 (2003).
- [22] I.M. Yaglom and V.G. Boltanskii. *Convex figures*, translated by P.J. Kelly and L.F. Walton, Holt, Rinehart and Winton (1961).
- [23] M. Yamanouti. Notes on closed convex sets. *Proceedings of the Physico-Mathematical Society of Japan Ser.* **14**: 605-609 (1932).

ECOLE NATIONALE SUPÉRIEURE DES MINES DE SAINT-ETIENNE, CIS - LPMG, UMR CNRS 5148, 158 COURS FAURIEL, 42023 SAINT-ETIENNE CEDEX 2, FRANCE, TEL.: +33-477-420219 / FAX: +33-477-499694,

E-mail address: rivollier@emse.fr ; debayle@emse.fr ; pinoli@emse.fr